
C H A P T E R - I I

PREPARATION OF FERRITES AND
X-RAY DIFFRACTION STUDIES

- (A) Method of Preparation
 - (B) X-ray Diffraction Studies
 - (C) Determination of Curie Temperature
-

(A) Method of Preparation

2.1 Introduction

Various preparation methods have been suggested by different workers for simple, mixed and substitutional ferrites^{1,2,3}.

We have prepared the ferrites by sintering of the oxides i.e. by ceramic method. This method offers ease of preparation, as the constituent oxides of high purity are readily available. The process of sintering is simple and the chances of impurity contaminating the resultant ferrites are also feeble.

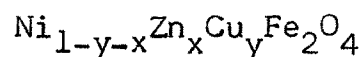
2.2 Mechanism of Solid State Reaction

The mechanism is discussed on the basis of diffusion of components involving divalent metal oxide MO and Fe_2O_3 . In the initial configuration there is only phase boundary between reactants. After the nucleation of the ferrite, the boundary is replaced by two different phase boundaries, one between MO and ferrite $\text{M Fe}_2\text{O}_4$ and the other between Fe_2O_3 and $\text{M Fe}_2\text{O}_4$. In this state further progress of the reaction can only take place by transport of reactants through the ferrite phase. Three different mechanisms of transfer in which $\text{M Fe}_2\text{O}_4$ may be found are discussed below. In the counter diffusion mechanism, first considered by Wagner^{5,6}, only cations migrate in the opposite directions, the oxygen ions are essentially stationary.

In the second model, the anions take part in the diffusion process. In this reaction diffusion of one cation is compensated by an associated flux of anions instead of a counter current of another cation. In the third mechanism, iron diffuses through the ferrite layer in a reduced state Fe^{2+} . In such a case oxygen is transported through the gas phase, being given off at $\text{M Fe}_2\text{O}_4/\text{Fe}_2\text{O}_3$ interface and taken up again at $\text{MO}/\text{M Fe}_2\text{O}_4$ boundary.

2.3 The General Formula

The general formula of our mixed ferrite system is



where

$x = 0, 0.2, 0.4, 0.6, 0.8, 1.0$ for $y = 0$.

and $x = 0, 0.2, 0.4, 0.6, 0.8$ for $y = 0.2$.

2.4 Raw Materials

AR grade Fe_2O_3 , ZnO , NiO and CuO supplied by Koch Light laboratories Ltd., Colnbrook Berks, England and Thomas Baker and Company London were used.

2.5 Weighing

The various oxides were weighed on a single pan microbalance of least count 10^{-5} gm and were mixed according to their molecular weight percentages.

2.6 Pre-sintering

Initially, the relevant oxides were taken in an agate mortar and were just mechanically blended in AR grade acetone base. The mixture was then allowed to dry in air and carefully transferred to a clean dry platinum crucible and presintered in a glo-bar furnace at 800°C for about 24 hours. The samples were then cooled in the furnace at the rate of 80°C per hour by reducing the current. The temperature of the furnace was measured by a chromel-alumel thermocouple along with a digital multimeter.

2.7 Grinding

The samples were then finally powdered by grinding for two to four^{hours} in an agate mortar using AR grade acetone. The samples were then sieved.

2.8 Sintering

The powders were then fired at 1200°C for about 40 hours. The temperature was slowly raised to the maximum value in order to maintain the final microstructure, content of oxygen, and the distribution of cations. The samples were cooled at the rate of 80°C per hour down to room temperature by reducing the current.

2.9 Pellet Formation

Finally, the samples were powdered and pellets of 1 cm diameter were formed by applying a pressure of 15 tons/inch² for about 15 minutes. 3 % solution of polyvenyl acetate (PVA) was used as the binder.

2.10 Final Sintering

The pellets were finally sintered at the highest temperature of 1200°C for twenty four hours. The temperature was increased slowly to ensure adequate supply of oxygen (air) to avoid the possibility of reduction of the samples. The samples were cooled at the rate of 80°C per hour down to room temperature. The pellets were finally polished smooth by a fine polish paper.

(B) X-Ray Diffraction Study

2.11 Introduction

To confirm the formation of the ferrite samples and characterisation of crystal structure we have used the x-ray diffraction technique. In this section the details of the diffractometer are furnished. The peaks of the diffractograms were indexed, the lattice constants and 'd' values were calculated. The results on the crystallographic data are briefly discussed.

2.12 The Diffractometer

In the present work Siemen's computerised diffractometer at Tata Institute of Fundamental Research, Bombay, was used.

The particulars are as follows:

1. Target used - Cu
2. Wavelength $\lambda = 1.54060 \text{ \AA}$
3. Rate of scanning - 2° per minute
4. Range of 2θ - 15° to 65°

5. Operating voltage - 40 kV
6. Operating current - 30 mA

Along with the diffractographs, the diffractometer furnished the following information.

1. Angular position of the peak - 2θ
2. The corresponding 'd' value as given by Bragg's relation
3. Height of the peak
4. Percentage height of the peak

2.13 Preparation of the Specimen

The specimen required for the diffractometer work was prepared in the following way. Very fine powder of the sample was pressed in the circular pit of diameter 1 cm of the holder and the surface was made perfectly plane by pressing the powder with a glass slide which when used in a skillful fashion resulted in a plane surface of the specimen. This was then placed in the sample holder. The samples were scanned between 15° to 65° and the first reflection was obtained at about $2\theta = 18^\circ$.

2.14 Indexing of the Peaks in the Diffraction Patterns

For a cubic lattice, the interplaner distance ' d_{hkl} ', lattice parameter 'a' and Miller indices h,k,l are related by⁷

$$d_{hkl} = \frac{a}{\sqrt{h^2 + k^2 + l^2}} \quad \dots \quad (2.1)$$

Bragg's law is

$$2 d_{hkl} \sin \theta_{hkl} = n\lambda$$

and for $n = 1$.

$$2 d_{hkl} \sin \theta_{hkl} = \lambda \quad \dots \quad (2.2)$$

The 'd' values are given along with '2 θ ' values by the computerised diffractometer.

The peak of 100 % height corresponds to the plane (311). So the lattice parameter 'a' in this case is calculated by using relation (2.1). For other peaks the h,k,l values were determined by the usual procedure⁸ and the peaks indexed.

A1 - NiFe₂O₄

Start at 2theta 15.000 Theta 7.500

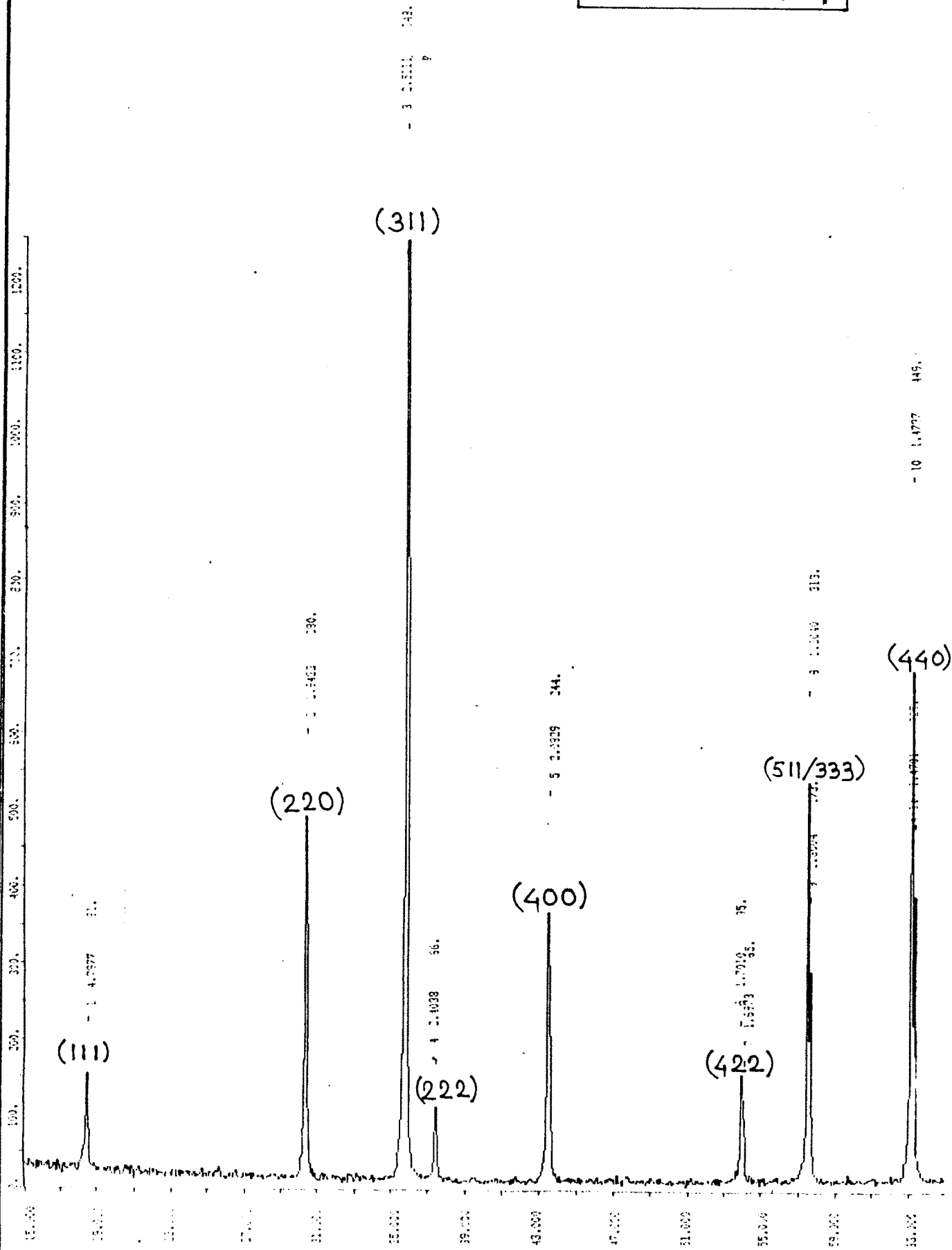


Fig. 2.1

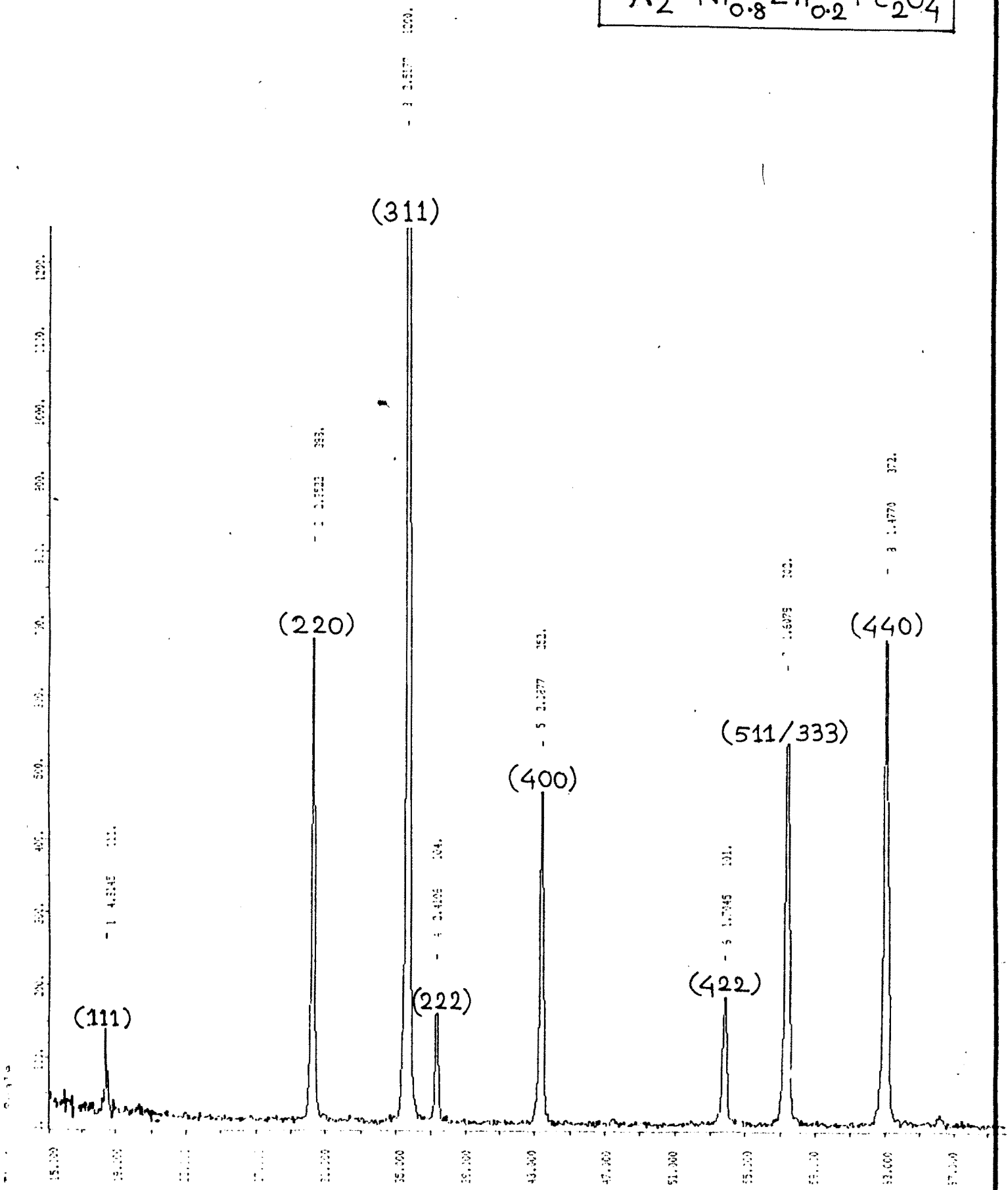
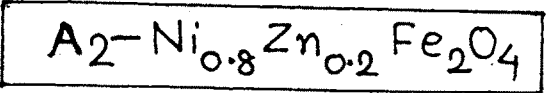


Fig. 2.2

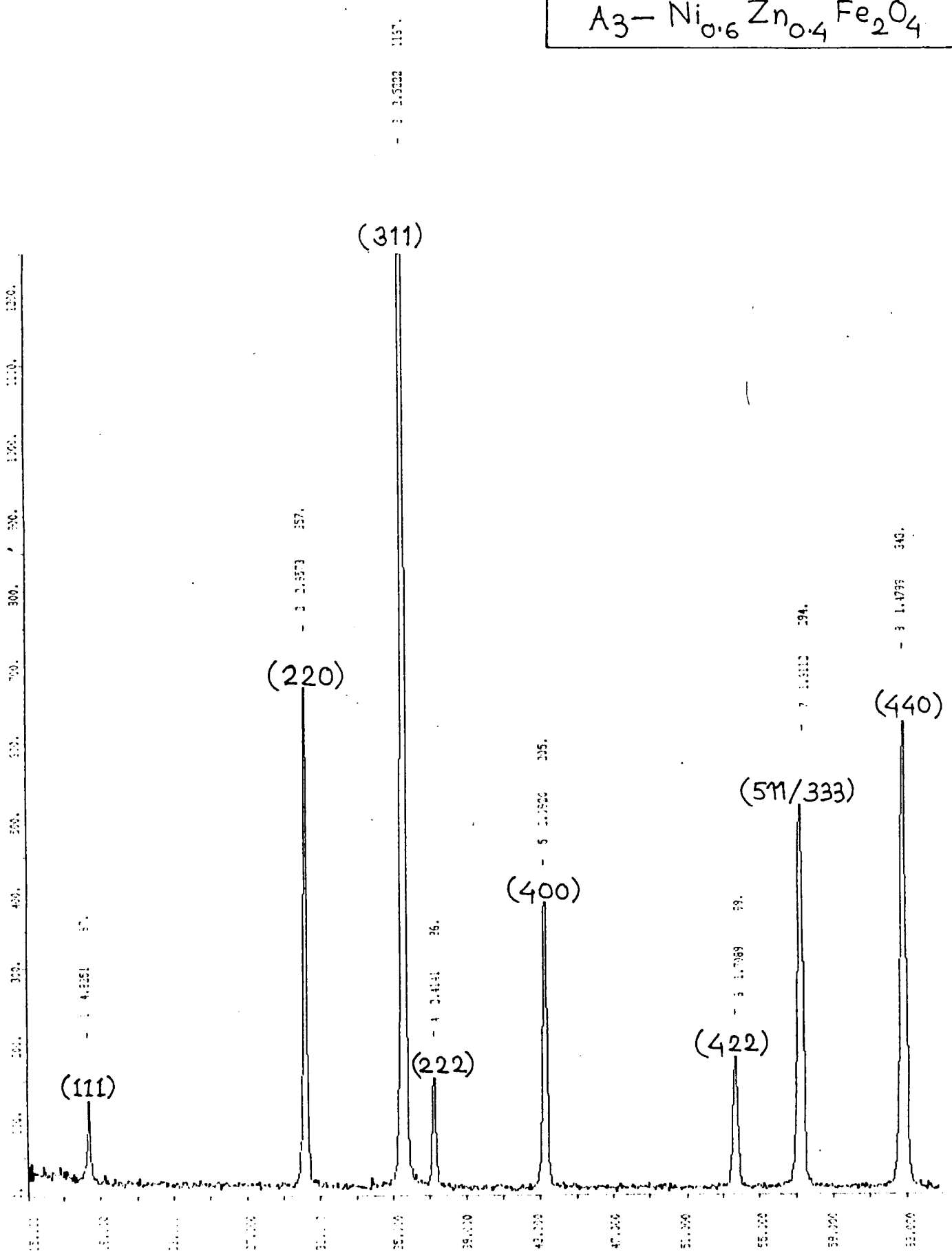
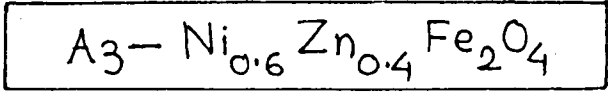


Fig. 2.3

1 POSITION 57--
 181973 4.8351
 HEIGHT X H.P.
 87. 7.5 111
 - 2 15 121X

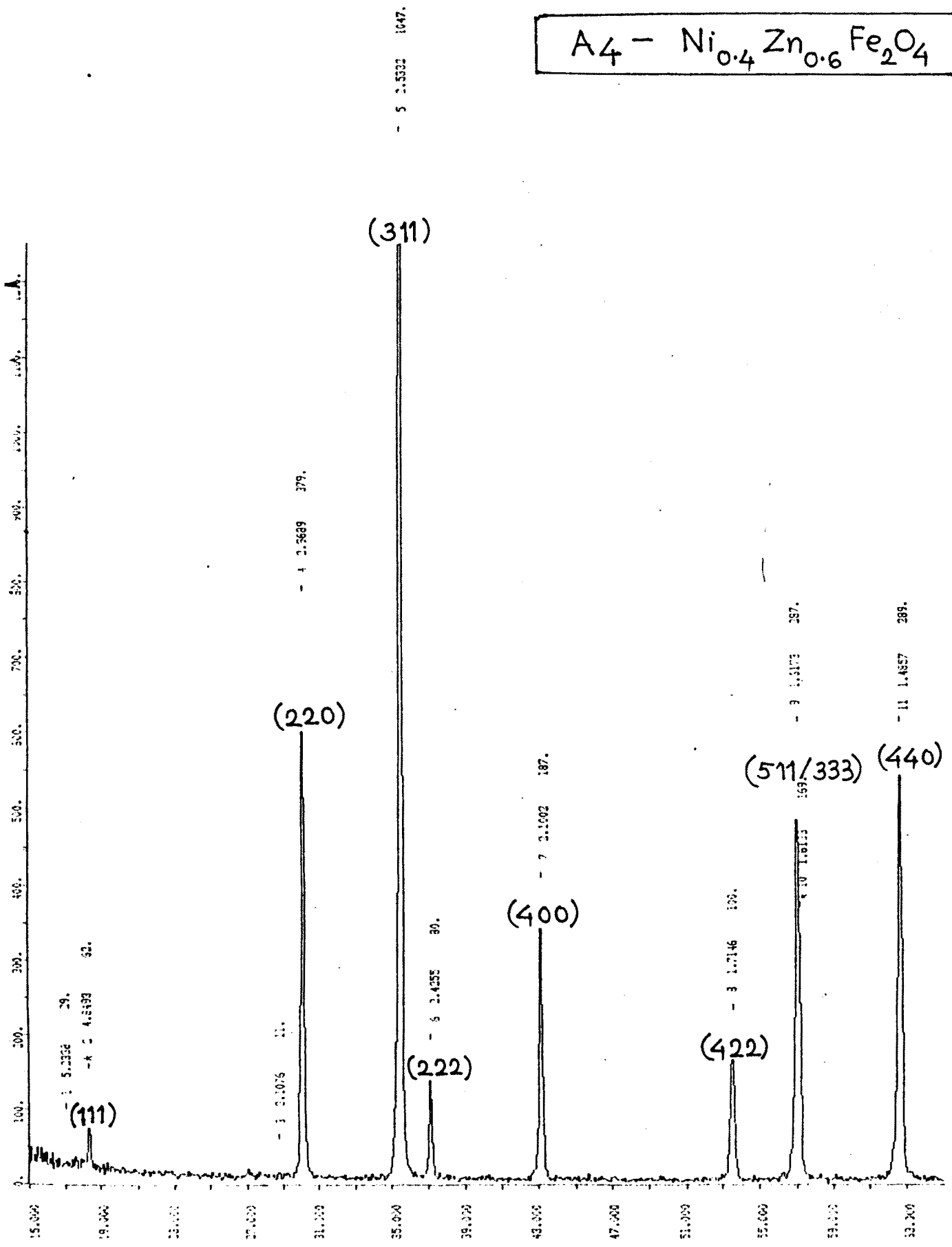
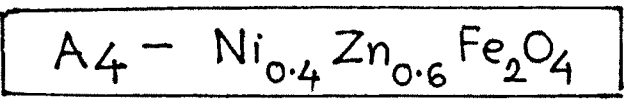
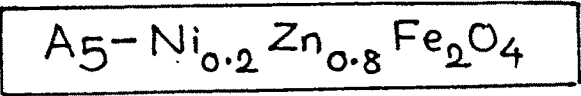


Fig. 2.4

POSITION	D/2	HEIGHT	H.P.
1	16.927	29.	2.8
2	18.780	27.	2.8



- 3 2.8397 1124.

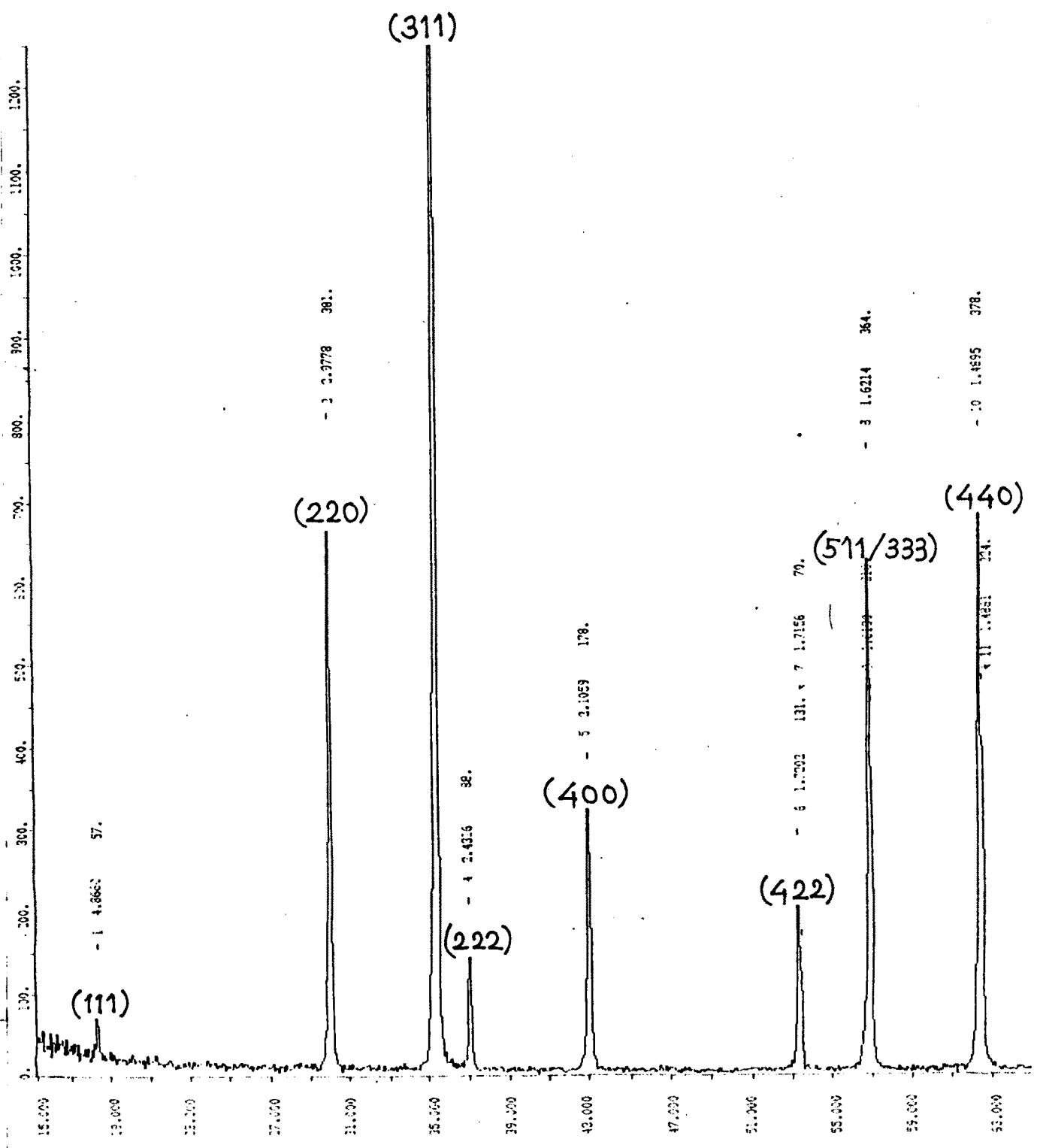


Fig. 2.5.

POSITION 0/ -- HEIGHT X H.P. 4.8 111
18.317 4.8660 57.

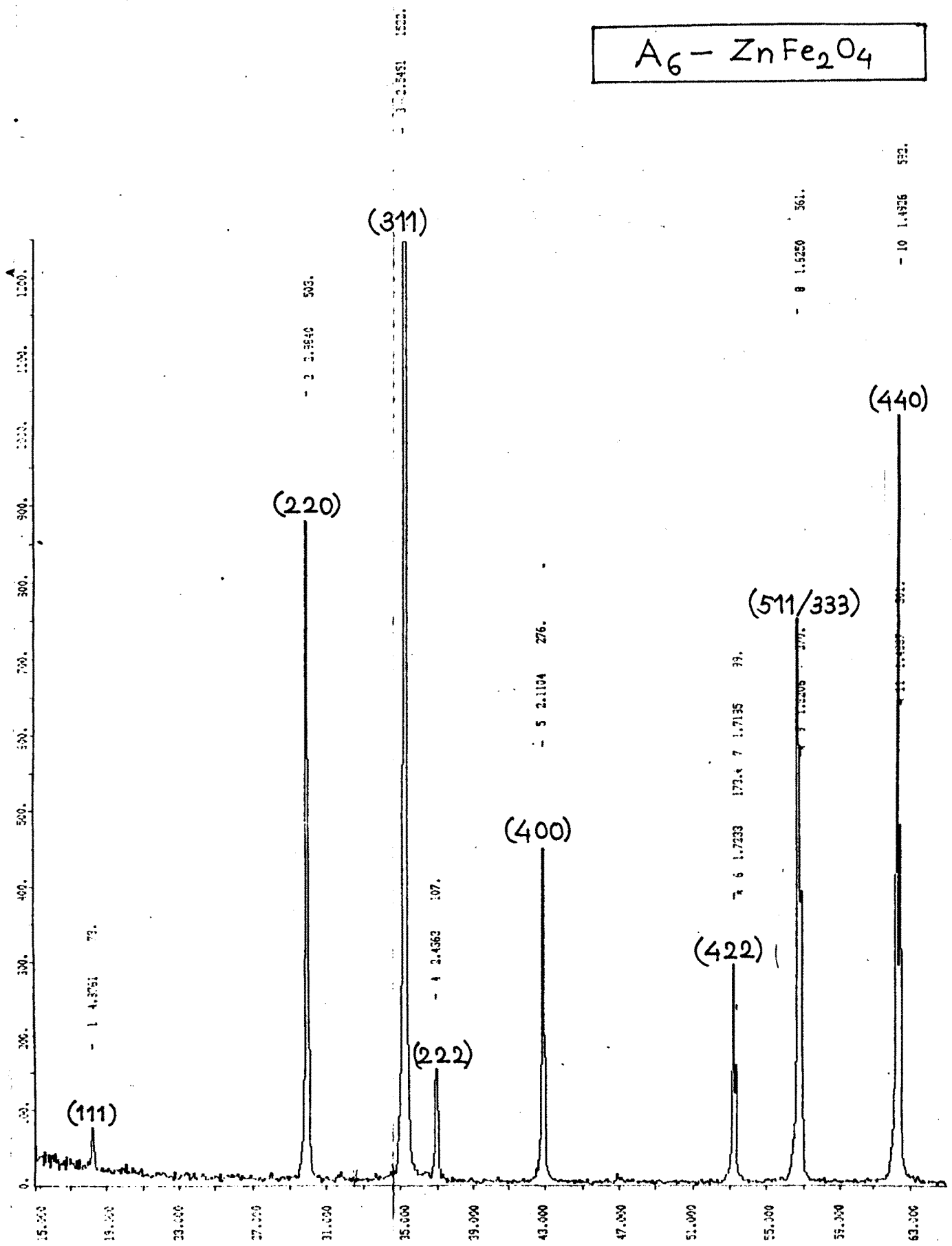
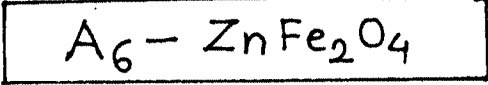


Fig. 2.6

POSITION 2θ --- HEIGHT % H.P.

29.919	2.9840	503
33.0	220	

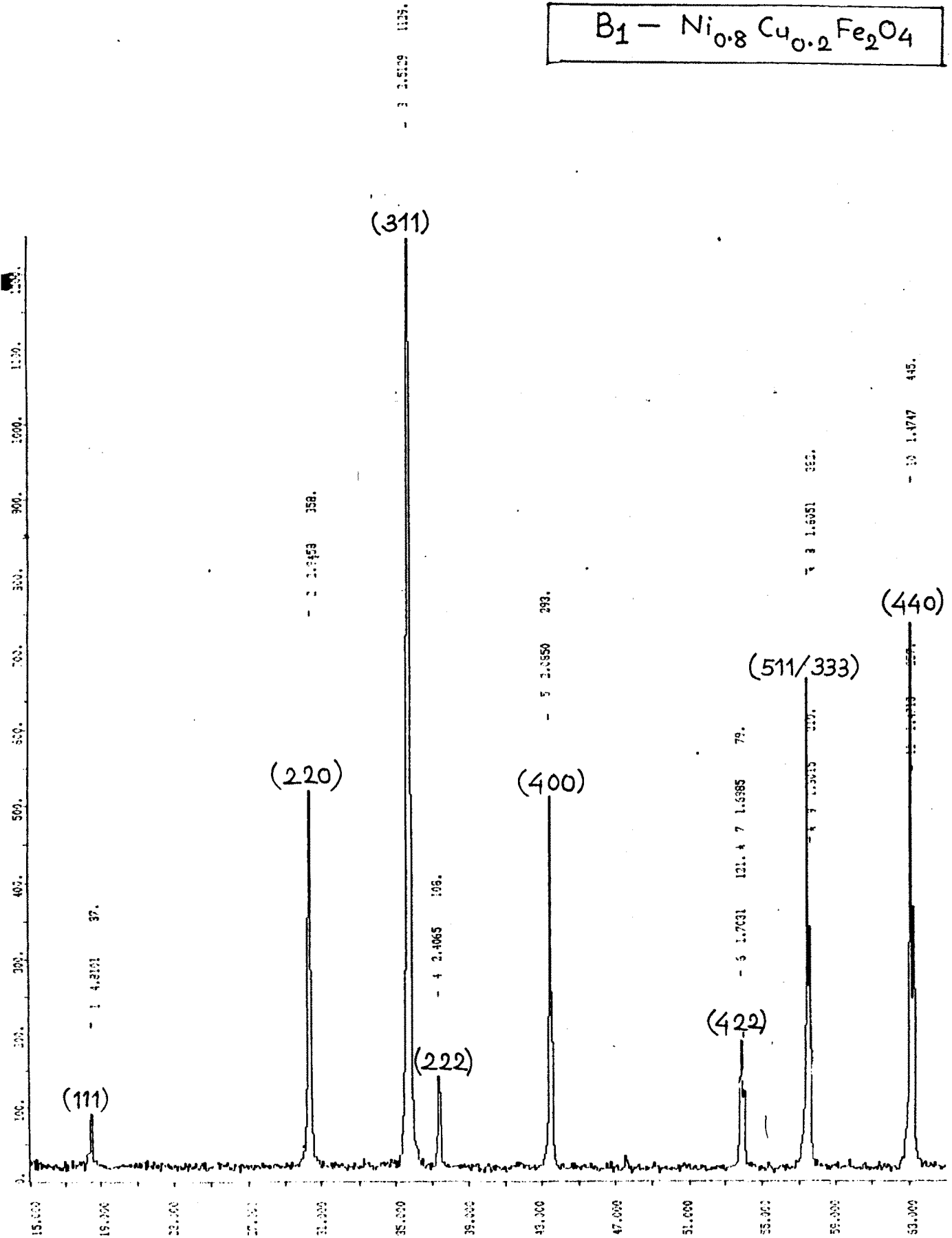
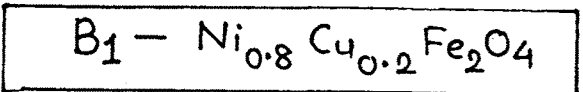


Fig. 2:7

2 30.317 2.945R
 37. 7.7 11
 45R. 31.7000

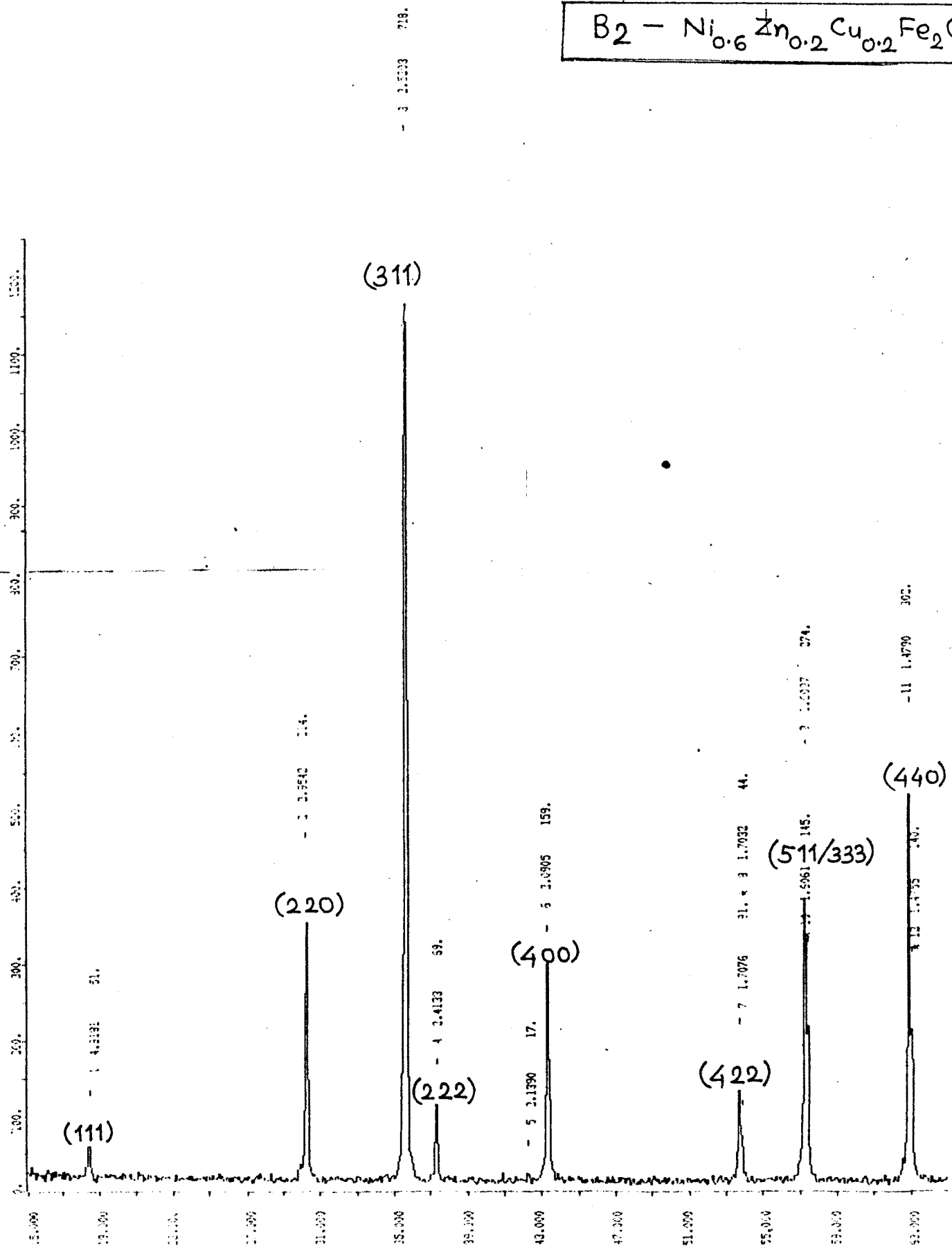
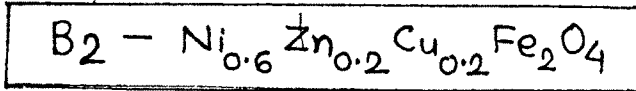


Fig. 2.8

POSITION 87--
 HEIGHT
 3 30.029 3.9542
 714. 78 8112

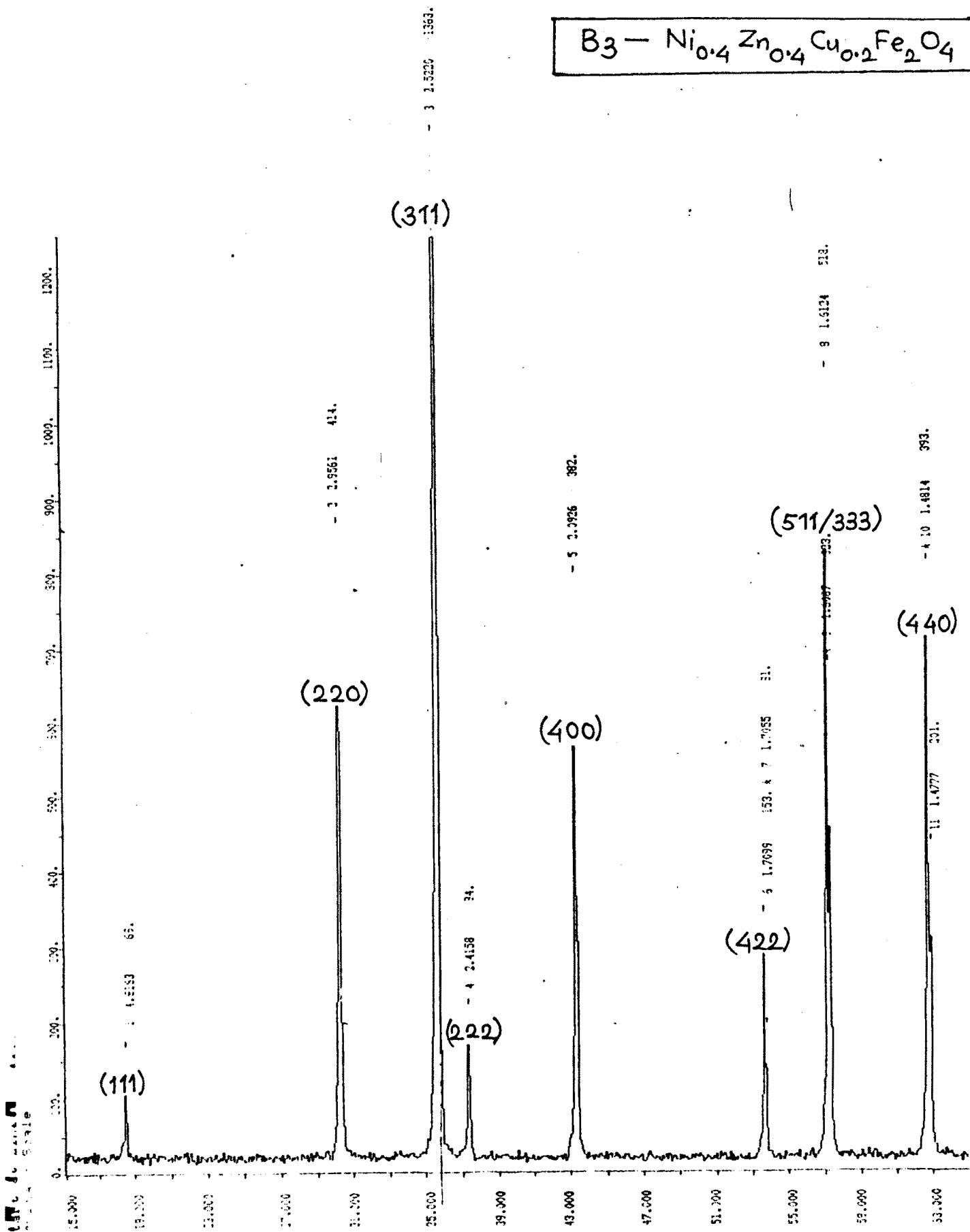
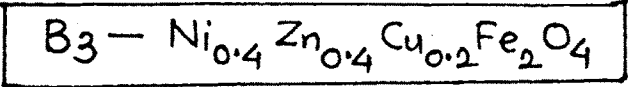
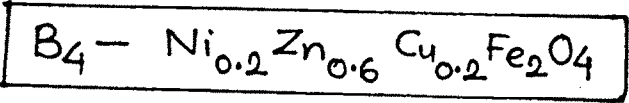


Fig. 2.9

1 18.407 4.8153 69. 5.1111
2 30.309 7.9561 414. 30.4900



M. time: 0.500, Step size: 0.020 155J
Start at 2theta 15.000 theta 7.500

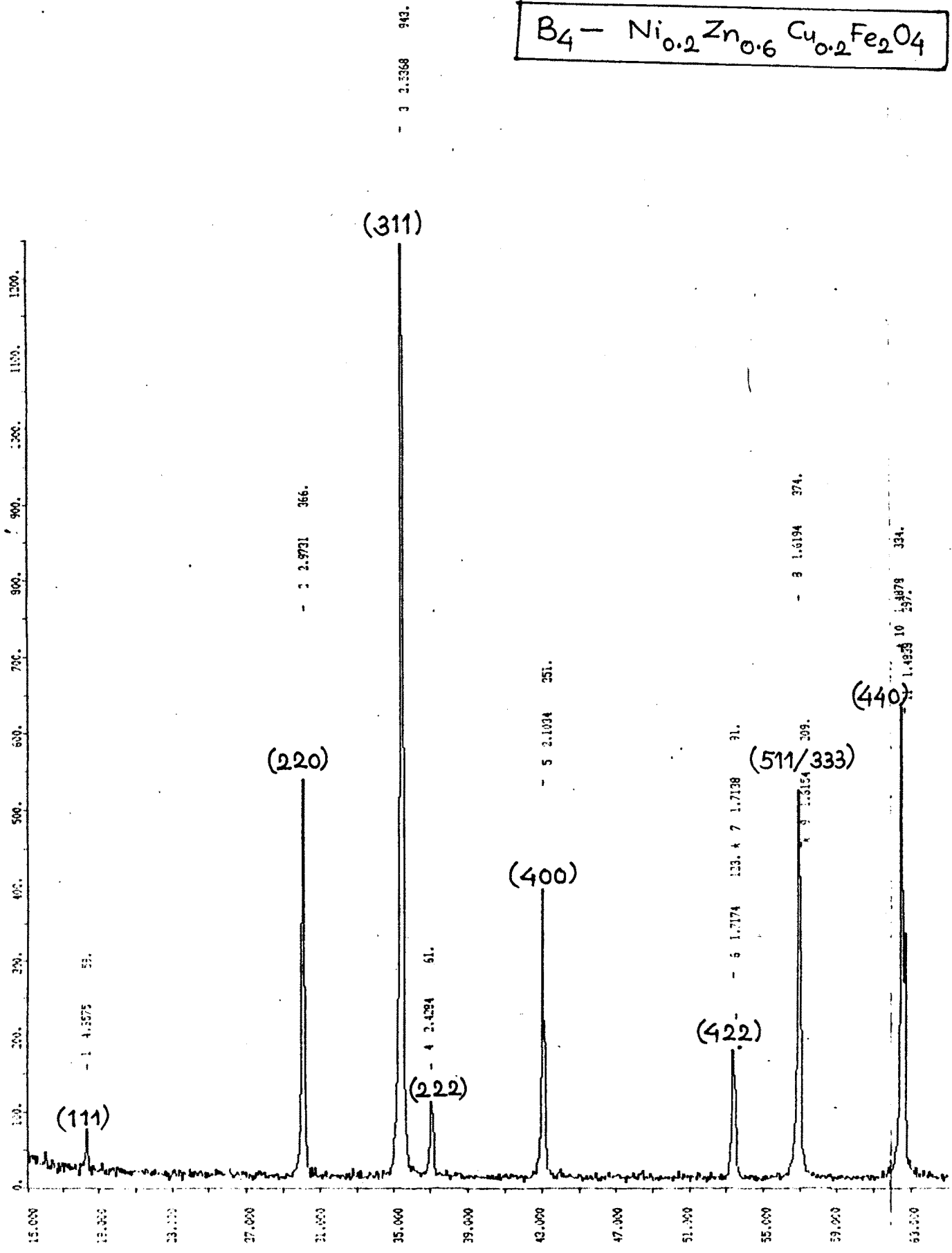


Fig. 2-10

POSITION D/2θ HEIGHT X H.P.

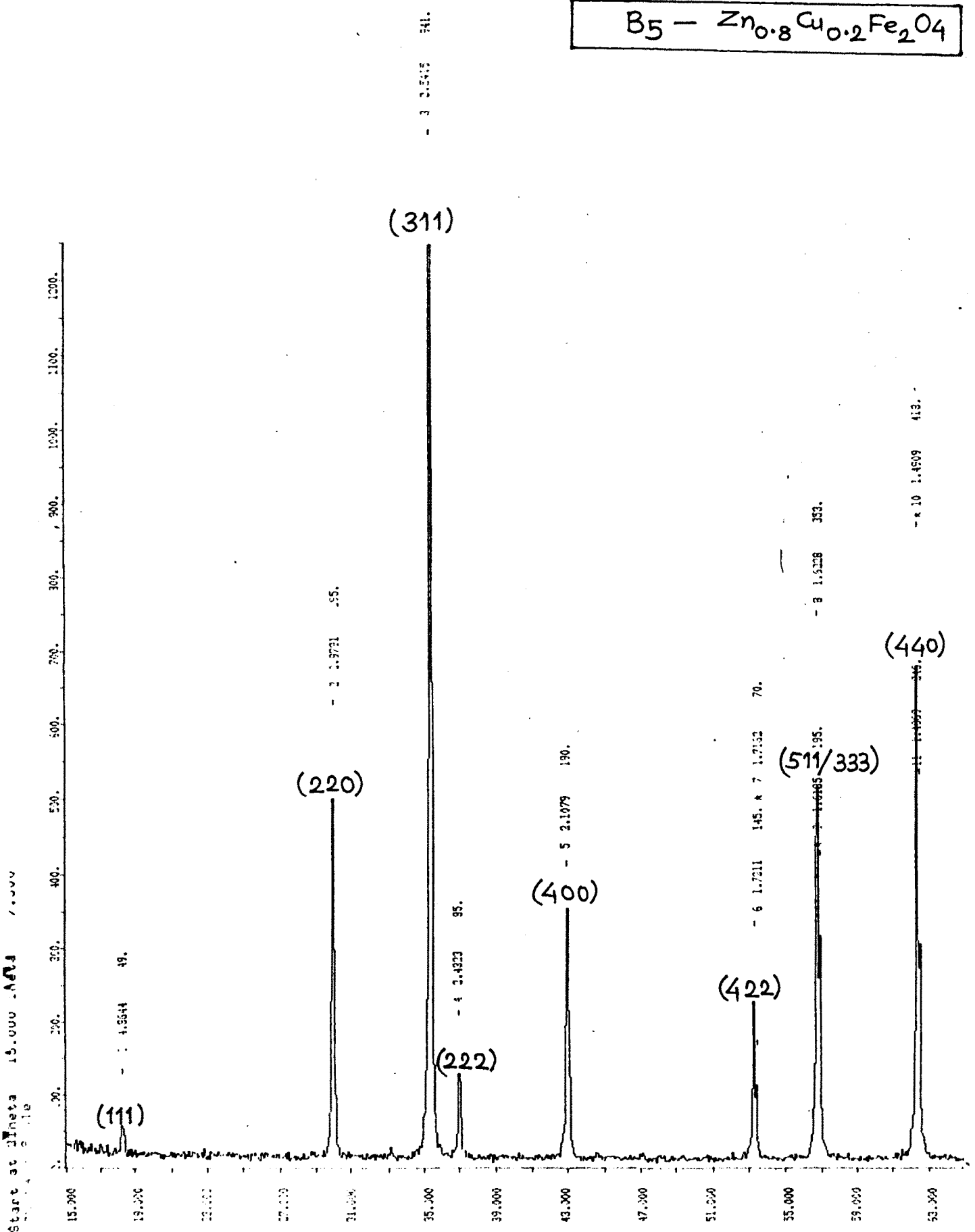
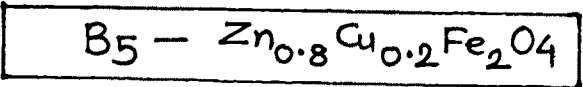


Fig. 2.11

POSITION 07-- HEIGHT x H.P. 49. 5.3 (11)

Table No. 2.1Sample A₁ - NiFe₂O₄

Sr.No. of peak	2 θ deg	d A ^o	d _{cal} A ^o	Plane hkl	a A ^o
1	18.478	4.7977	4.8121	111	8.3099
2	30.335	2.9422	2.9468	220	8.3218
3	35.727	2.5111	2.5130	311	8.3284
4	37.380	2.4038	2.4060	222	8.3270
5	43.410	2.0829	2.0837	400	8.3316
6	53.855	1.7010	1.7013	422	8.3332
7	57.402	1.6040	1.6040	511/333	8.3346
8	63.028	1.4737	1.4734	440	8.3365

$$a = 8.3350 \text{ A}^{\circ}$$

Table No. 2.2Sample A₂ - Ni_{0.8}Zn_{0.2}Fe₂O₄

Sr.No. of peak	2 θ deg	d A ^o	d _{cal} A ^o	Plane hkl	a A ^o
1	18.413	4.8145	4.8227	111	8.3389
2	30.250	2.9522	2.9533	220	8.3500
3	35.631	2.5177	2.5186	311	8.3502
4	37.271	2.4106	2.4114	222	8.3505
5	43.305	2.0877	2.0883	400	8.3508
6	53.733	1.7045	1.7051	422	8.3503
7	57.253	1.6078	1.6076	511/333	8.3543
8	62.872	1.4770	1.4767	440	8.3551

$$a = 8.3532 \text{ A}^{\circ}$$

Table No. 2.3Sample A₃ - Ni_{0.6}Zn_{0.4}Fe₂O₄

Sr.No. of peak	2 θ deg.	d A ^o	d _{cal} A ^o	Plane hkl	a A ^o
1	18.373	4.8251	4.8334	111	8.3573
2	30.197	2.9573	2.9599	220	8.3645
3	35.565	2.5222	2.5242	311	8.3652
4	37.215	2.4141	2.4167	222	8.3627
5	43.210	2.0920	2.0929	400	8.3680
6	53.586	1.7089	1.7089	422	8.3718
7	57.121	1.6112	1.6112	511/333	8.3720
8	62.732	1.4799	1.4799	440	8.3715

$$a = 8.3718 \text{ A}^{\circ}$$

Table No. 2.4Sample A₄ - Ni_{0.4}Zn_{0.6}Fe₂O₄

Sr.No. of peak	2 θ deg.	d _o A ^o	d _{cal} A ^o	Plane hkl	a A ^o
1	18.280	4.8493	4.8511	111	8.3992
2	30.076	2.9689	2.9707	220	8.3973
3	35.405	2.5332	2.5332	311	8.4016
4	37.034	2.4255	2.4256	222	8.4021
5	43.035	2.1002	2.1006	400	8.4008
6	53.391	1.7146	1.7151	422	8.3998
7	56.886	1.6173	1.6170	511/333	8.4037
8	62.462	1.4857	1.4853	440	8.4043

$$a = 8.4024 \text{ A}^{\circ}$$

Table No. 2.5Sample A₅ - Ni_{0.2}Zn_{0.8}Fe₂O₄

Sr.No. of peak	2 θ deg.	d A ^o	d _{cal} A ^o	Plane hkl	a A ^o
1	18.217	4.8660	4.8648	111	8.4281
2	29.983	2.9778	2.9790	220	8.4224
3	35.312	2.5391	2.5405	311	8.4232
4	36.938	2.4316	2.4324	222	8.4233
5	42.912	2.1059	2.1065	400	8.4236
6	53.206	1.7202	1.7200	422	8.4272
7	56.730	1.6214	1.6216	511/333	8.4250
8	62.285	1.4895	1.4895	440	8.4258

$$a = 8.4260 \text{ A}^{\circ}$$

Table No. 2.6Sample A₆ - ZnFe₂O₄

Sr.No. of peak	2 θ deg	d A ^o	d _{cal} A ^o	plane hkl	a A ^o
1	18.179	4.8761	4.8747	111	8.4456
2	29.919	2.9840	2.9851	220	8.4400
3	35.234	2.5451	2.5457	311	8.4411
4	36.863	2.4363	2.4373	222	8.4396
5	42.816	2.1104	2.1008	400	8.4416
6	53.100	1.7233	1.7325	422	8.4424
7	56.591	1.6250	1.6249	511/333	8.4437
8	62.141	1.4926	1.4926	440	8.4434

$$a = 8.4432 \text{ A}^{\circ}$$

Table No. 2.7

Sample **B**₁ - Ni_{0.8}Cu_{0.2}Fe₂O₄

Sr.No. of peak	2 θ deg	d A ^o	d _{cal} A ^o	plane hkl	a A ^o
1	18.430	4.8101	4.8162	111	8.3313
2	30.317	2.9458	2.9493	220	8.3320
3	35.701	2.5129	2.5152	311	8.3343
4	37.337	2.4065	2.4081	222	8.3364
5	43.363	2.0850	2.0855	400	8.3400
6	53.783	1.7031	1.1988	422	8.3435
7	57.360	1.6051	1.6054	511/333	8.3403
8	62.982	1.4747	1.4747	440	8.3421

$$a = 8.3420 \text{ A}^{\circ}$$

Table No. 2.8

Sample **B**₂ - Ni_{0.6}Zn_{0.2}Cu_{0.2}Fe₂O₄

Sr.No. of peak	2 θ deg	d A ^o	d _{cal} A ^o	plane hkl	a A ^o
1	18.399	4.8181	4.8298	111	8.3452
2	30.229	2.9542	2.9576	220	8.3557
3	35.593	2.5203	2.5223	311	8.3589
4	37.228	2.4133	2.4149	222	8.3599
5	43.244	2.0905	2.0914	400	8.3620
6	53.630	1.7076	1.7076	422	8.3655
7	57.159	1.6097	1.6099	511/333	8.3642
8	62.777	1.4790	1.4788	440	8.3665

$$a = 8.3654 \text{ A}^{\circ}$$

Table No. 2.9

Sample - $B_3 - Ni_{0.4}Zn_{0.4}Cu_{0.2}Fe_2O_4$

Sr.No. of peak	2θ deg	d \AA°	d_{cal} \AA°	plane hkl	a \AA°
1	18.407	4.8163	4.8373	111	8.3420
2	30.209	2.9561	2.9622	220	8.3611
3	35.569	2.5220	2.5262	311	8.3645
4	37.187	2.4158	2.4186	222	8.3686
5	43.198	2.0926	2.0946	400	8.3704
6	53.552	1.7099	1.7082	422	8.3768
7	57.076	1.6125	1.6124	511/333	8.3783
8	62.660	1.4814	1.4810	440	8.3800

$$a = 8.3784 \text{ \AA}^\circ$$

Table No. 2.10

Sample $B_4 - Ni_{0.2}Zn_{0.6}Cu_{0.2}Fe_2O_4$

Sr.No. of peak	2θ deg	d \AA°	d_{cal} \AA°	plane hkl	* a \AA°
1	18.249	4.8575	4.8583	111	8.4134
2	30.033	2.9731	2.9751	220	8.4092
3	35.355	2.5368	2.5372	311	8.4136
4	36.989	2.4284	2.4291	222	8.4122
5	42.956	2.1034	2.1037	400	8.4136
6	53.298	1.7174	1.7177	422	8.4135
7	56.806	1.6194	1.6199	511/333	8.4146
8	62.360	1.4878	1.4875	440	8.4163

$$a = 8.4148 \text{ \AA}^\circ$$

Table No. 2.11

Sample **B**₅ - $\text{Zn}_{0.8}\text{Cu}_{0.2}\text{Fe}_2\text{O}_4$

Sr.No. of peak	2θ deg	d \AA°	d_{cal} \AA°	plane hkl	a \AA°
1	18.223	4.8644	4.8685	111	8.4254
2	29.970	2.9791	2.9814	220	8.4262
3	35.286	2.5415	2.5425	311	8.4292
4	36.926	2.4343	2.4343	222	8.4327
5	42.869	2.1079	2.1081	400	8.4316
6	53.174	1.7211	1.7213	422	8.4316
7	56.677	1.6228	1.6228	511/333	8.4323
8	62.220	1.4909	1.4007	440	8.4338

$$a = 8.4326 \text{ \AA}^\circ$$

Table No. 2.12

Ferrite sample	lattice parameter a in \AA°	Δa \AA°
A ₁ NiFe_2O_4	8.3350	
A ₂ $\text{Ni}_{0.8}\text{Zn}_{0.2}\text{Fe}_2\text{O}_4$	8.3530	
A ₃ $\text{Ni}_{0.6}\text{Zn}_{0.4}\text{Fe}_2\text{O}_4$	8.3718	
A ₄ $\text{Ni}_{0.4}\text{Zn}_{0.6}\text{Fe}_2\text{O}_4$	8.4024	
A ₅ $\text{Ni}_{0.2}\text{Zn}_{0.8}\text{Fe}_2\text{O}_4$	8.4260	
A ₆ ZnFe_2O_4	8.4432	
B ₁ $\text{Ni}_{0.8}\text{Cu}_{0.2}\text{Fe}_2\text{O}_4$	8.3420	0.0070 \approx .01
B ₂ $\text{Ni}_{0.6}\text{Zn}_{0.2}\text{Cu}_{0.2}\text{Fe}_2\text{O}_4$	8.3654	0.0124 \approx .01
B ₃ $\text{Ni}_{0.4}\text{Zn}_{0.4}\text{Cu}_{0.2}\text{Fe}_2\text{O}_4$	8.3784	0.0066 \approx .01
B ₄ $\text{Ni}_{0.2}\text{Zn}_{0.6}\text{Cu}_{0.2}\text{Fe}_2\text{O}_4$	8.4148	0.0124 \approx .01
B ₅ $\text{Zn}_{0.8}\text{Cu}_{0.2}\text{Fe}_2\text{O}_4$	8.4326	0.0066 \approx .01

2.15 Results and Discussion

The diffraction maxima were indexed and the indices tallied with those expected for spinel structure⁸. The reflections observed are (111), (220), (311), (222), (400), (422), (511) or (333) and (440). These correspond to the allowed values of reflections for cubic spinel structure⁸. The observed and calculated d values, Miller indices along with lattice parameter are presented in the tables (Table No. 2.1 to 2.11) and the compositionwise lattice parameter in Table 2.12.

Fig.(2.12) shows the compositional variation of the lattice parameter 'a' in A° with the content of zinc for the ferrite system $\text{Ni}_{1-x}\text{Zn}_x\text{Fe}_2\text{O}_4$

It is seen that the lattice parameter increases in an almost linear fashion with the addition of zinc. The lattice parameter is minimum for NiFe_2O_4 (8.3350 A°) and maximum for ZnFe_2O_4 (8.4432 A°). These values of 'a' for NiFe_2O_4 and ZnFe_2O_4 are in close agreement with those reported earlier^{9,10}. The increase in the lattice parameter with the content of zinc shows that Vegards' law is obeyed by the compositional variation 'a'. Similar behaviour is observed for the ferrite system $\text{Ni}_{0.8-x}\text{Zn}_x\text{Cu}_{0.2}\text{Fe}_2\text{O}_4$ which is shown in figure No.2.13.

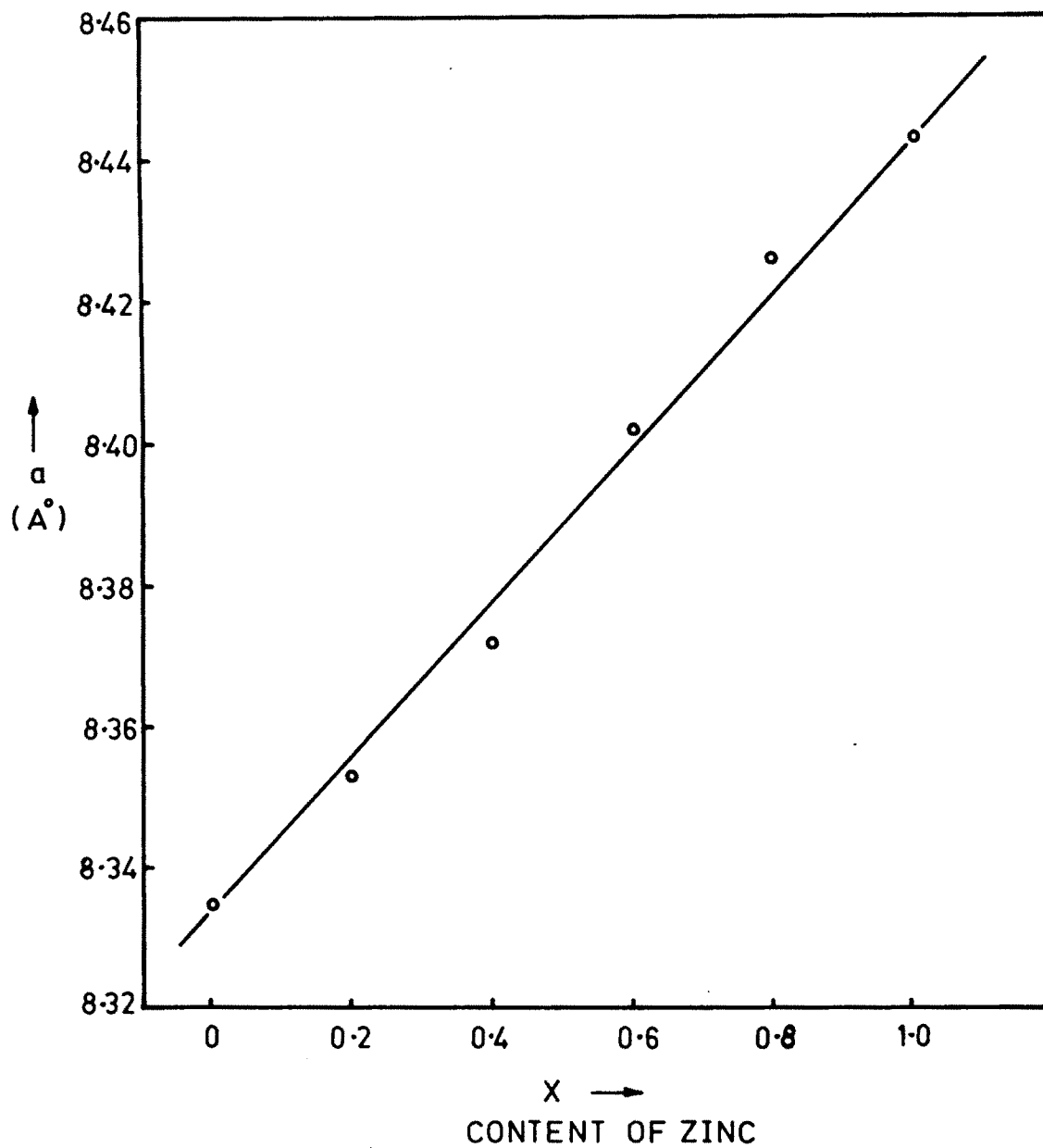


Fig.2-12: VARIATION OF LATTICE PARAMETER (a) WITH CONTENT OF ZINC (x) FOR $\text{Ni}_{1-x}\text{Zn}_x\text{Fe}_2\text{O}_4$.

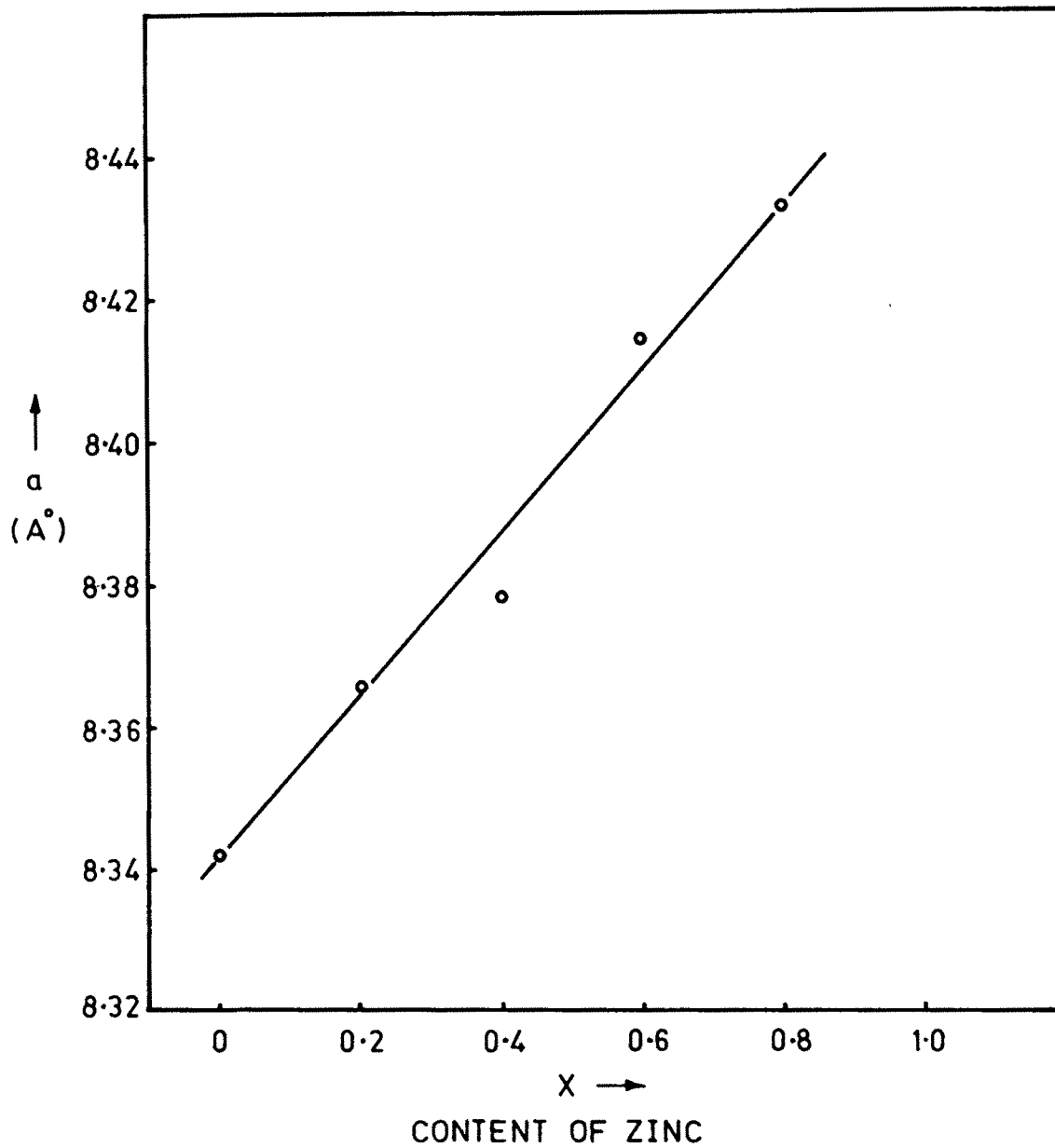


Fig. 2-13 : VARIATION OF LATTICE PARAMETER (a) WITH CONTENT OF ZINC (X) FOR $\text{Ni}_{8-x}\text{Zn}_x \text{Cu}_{0.2}\text{Fe}_2\text{O}_4$.

Table No. 2.13

Ion	Cu ⁺⁺	Ni ⁺⁺	Zn ⁺⁺
Ionic Radius	0.70 A ^o	0.74 A ^o	0.83 A ^o

In table No.2.13 the ionic radii for Zn⁺⁺, Cu⁺⁺, and Ni⁺⁺ are shown with the addition of zinc the Ni⁺⁺ ion is replaced which has smaller ionic radius than the zinc. Thus the lattice parameter shows an increase.

In table 2.12 the change in the lattice parameter 'a' i.e. **Aa** with the addition of copper in NiZn ferrite is shown. It is seen that, in general, the lattice parameter shows a decrease with the addition of 0.2 copper. Within the experimental error, when the ferrites containing same content of zinc in both the systems are compared, the lattice parameter does not show either increasing or decreasing trend. The deviation in the lattice parameter is approximately 0.01 A^o, for all the copper containing Ni-Zn ferrites. The deviation in the lattice parameter can again be explained on the basis of ionic volume of the copper ion, which in this case, is replacing Zn ion. The ionic radius of Cu⁺⁺ is 0.70 A^o while that of Zn⁺⁺ is 0.83 A^o. Also copper is a temperature sensitive and Jahn-Teller ion and its presence may be causing Jahn Teller distortion contracting the cell size.



The samples of NiZn ferrite system and copper substituted Ni-Zn ferrite system exhibited a cubic structure which is in agreement with that reported by Patani et al.¹¹

Thus when the zinc is replaced by copper the lattice constant of the sample decreases which may be attributed to the smaller diameter of copper ion than the zinc ion, and its Jahn-Tellor distortion effect.

Cu^{++} is a Jahn-Tellor ion and copper ferrite shows a tetragonal structure which is attributed to the presence of Cu^{++} ions on B sites¹². In our system the possibility of Cu^{++} ions migrating to A site cannot be ruled out, however the presence of Cu^{++} ions on B site may be sufficient to cause tetragonal distortion of the lattice.

2.16 Apparatus and Determination of Curie Temperatures

We have evaluated the Curie temperatures of our samples by the technique which is described below in detail. Loria et al¹³ have suggested a method of determination of Curie temperatures. We have modified this technique. The method by Loria et al. suffers from a draw back, that along with the pellet the core of the electromagnet is also subjected to heating, which causes a damage to the enamel of the electromagnet wire, leading to short circuit. At the same time more current is required to obtain substantial magnetisation. We have improved upon the

technique, by not directly subjecting the core of the electromagnet to the temperature of the furnace, instead induction technique is used for magnetising the specimen bar to which the pellet is attached. Accurate measurement of the Curie temperature is made by using a chromel alumel thermocouple along with a digital multimeter of least count 0.1 mV enabling measurement of temperature correctly upto 2.5°C. Fig.2.14 shows this technique.

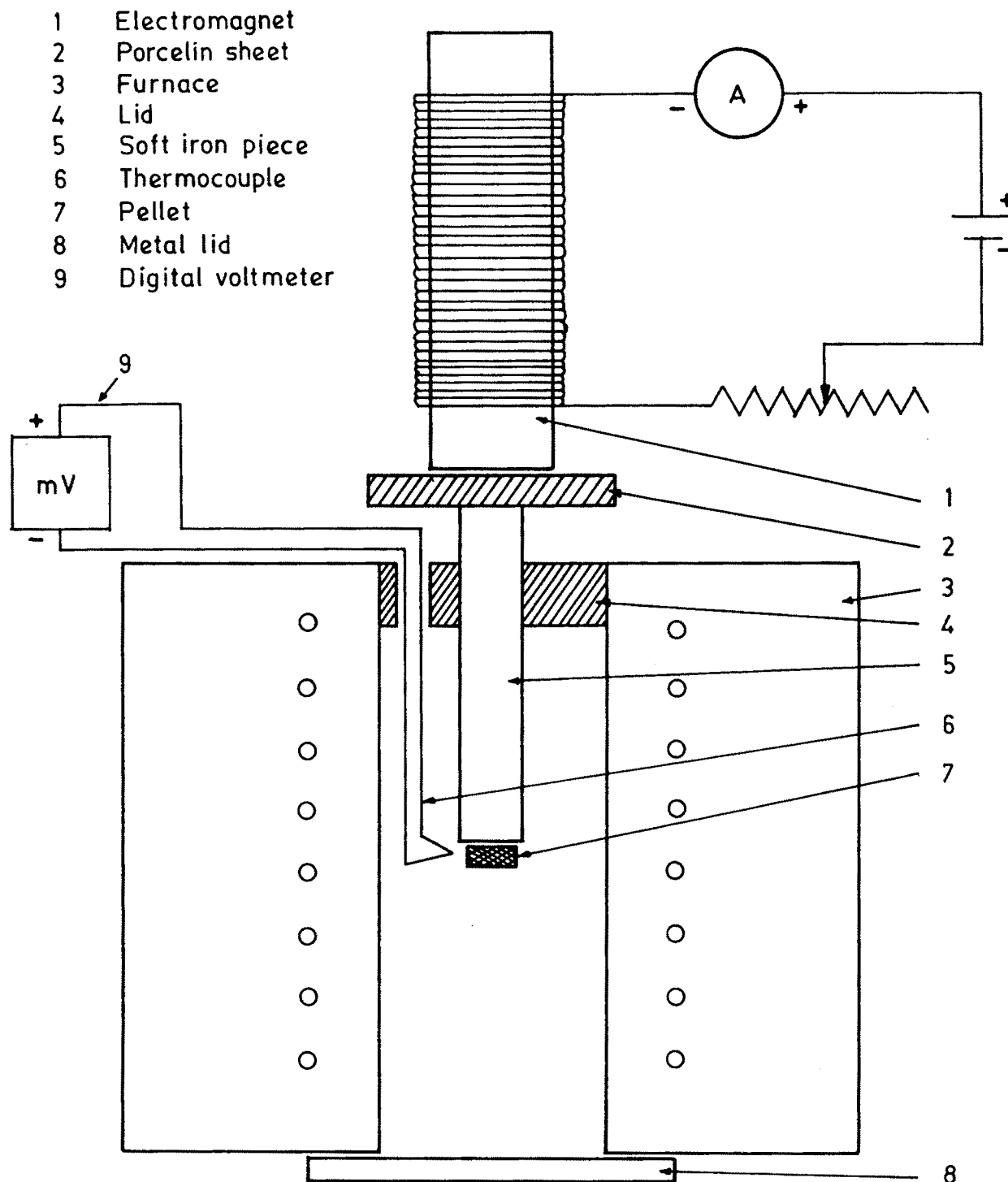


Fig. 2-14 : SET UP FOR DETERMINATION OF CURIE TEMPERATURE (T_c).

Table No. 2.13

Ferrite	Curie temperature T_c °K	
A_1	$NiFe_2O_4$	907
A_2	$Ni_{0.8}Zn_{0.2}Fe_2O_4$	805
A_3	$Ni_{0.6}Zn_{0.4}Fe_2O_4$	698
A_4	$Ni_{0.4}Zn_{0.6}Fe_2O_4$	553
A_5	$Ni_{0.2}Zn_{0.8}Fe_2O_4$	473
A_6	$ZnFe_2O_4$	-
B_1	$Ni_{0.8}Cu_{0.2}Fe_2O_4$	868
B_2	$Ni_{0.6}Zn_{0.2}Cu_{0.2}Fe_2O_4$	766
B_3	$Ni_{0.4}Zn_{0.4}Cu_{0.2}Fe_2O_4$	644
B_4	$Ni_{0.2}Zn_{0.6}Cu_{0.2}Fe_2O_4$	482
B_5	$Zn_{0.8}Cu_{0.2}Fe_2O_4$	-

References

- 1) Toshio Takada and M.Kiyamgi, Ferrites, Proces. Internat. Conf.(July 1970), Japan, pp.69-71.
- 2) Donald,G.Wickham, Ferrites, Proces.Internat.Conf.(July 1970), Japan, pp 105-107.
- 3) Toshihito Sata, Chinji Kuroda and Minoru Sato, Ferrites, Proces. Internat. Conf. (July (1970), Japan, pp.72-74.
- 4) G.Economous, J.Ama.Cera.Soc. 38 (1955) p. 241.
- 5) C.Wagner, Z.Phys.Chem. B-34, (1936) p.309-316.
- 6) C.G.Kaczynski, Internat.Conf.(1970), Japan, pp.87-95.
- 7) Henry,N.F.M., Lipson H. and Wooster,W.A., The interpretation of X-ray diffraction photographs, Macmillan and Co.Ltd., London (1961).
- 8) B.D.Culley, Elements of X-ray diffraction, Addison Wesley Publishing Co., Inc.England (1959).
- 9) H.V.Kiran, A.L.Shashimohan, D.K.Chakrabarty and A.B.Biswas, Phys.Stat.Sol (A) 66, (1981), p.743.
- 10) N.S.Satyamurthy, M.G.Natera and S.I. Youseff^S_A, Phys.Rev., 181 (1969) p.969.
- 11) C.M.Srivastava, M.J.Patani and T.T.Srinivasan, J.Appl. Phys. 53(3) (1982), p.2107.

- 12) Belov K.P., Goryaga A.N., Antoshina L.G., Sovt.Phys. Solid State (USA) 15 (1974) p.1935.
- 13) Kamazin A.S., Fiz Tverd Tela (USSR) 17 (1975) p.2419.
- 14) V.U.Patil, Kulkarni R.G., Solid Stat.Comn. 31 (1979) p.551.
- 15) E.M.Shrivastava, G.Shrinivasan, N.G. Nanadikar, Phys. Rev., B 19 (1979) p.499.
- 16) K.K. Loria, A.P.B.Sinha, Ind.J.Pure and Applied Phys., 1 (1963) p. 215.